SCIENTIFIC REPORTS

OPEN

SUBJECT AREAS:
GEOCHEMISTRY
BIOGEOCHEMISTRY
MARINE CHEMISTRY

Received
28 May 2014

Accepted
10 July 2014

Published
28 July 2014

Correspondence and requests for materials should be addressed to C.-L.L. (linnohc@fac.nsysu.edu.tw)

Carbonaceous particles reduce marine microgel formation

Ruei-Feng Shiu[1], Wei-Chun Chin[2] & Chon-Lin Lee[1,3]

[1]Department of Marine Environment and Engineering, National Sun Yat-sen University, 80424 Kaohsiung, Taiwan, ROC, [2]School of Engineering, University of California at Merced, Merced, California, USA, [3]Kuroshio Research Group, Asia-Pacific Ocean Research Center, National Sun Yat-sen University, 80424 Kaohsiung, Taiwan, ROC.

An increase in ambient carbonaceous particle (CNP) levels has been found, potentially leading to significant environmental/health hazards. These particles will ultimately enter the oceanic environment and interact with dissolved organic carbon. However, a detailed mechanistic understanding of their behavior, transport, and fate in marine systems is still much needed. This study, using carbon black (CB, 14 nm) nanoparticles as a model, aimed to investigate the impact of CNPs on marine microgel formation, a critical shunt between DOC and particulate organic carbon that potentially represents a ~70-Gt organic carbon flux. We found that CB can enhance the stability of DOC polymers and reduce microgel equilibrium sizes in concentration as low as 1 μgL^{-1} CB, possibly due to negative surface charges on CB that decrease cross-linking bridges through Ca^{2+} bonds. The reduction of marine microgel formation induced by CB could lead to a decrease in the downward transportation of microbial substrates and nutrients, and therefore, could have a significant impact on the carbon cycle and the marine ecosystem.

Marine dissolved organic carbon, a massive reservoir of reduced carbon[1,2], plays a critical role in biologically-mediated carbon cycling, which accounts for a total mass of ~700 Gt (7×10^{17} grams) of carbon[3]. About 50% of the photosynthetic production by surface phytoplankton or bacteria is released as DOC biopolymers such as exopolymeric substances (EPS) and other biological secretions into the DOC pool[4]. It was previously estimated that around 10% of DOC polymers can self-assemble to form the matrix of microscopic hydrogels, containing ~70 Gt of carbon[5–7]. The microgel formation is critical because these organic polymers not only can selectively transport bioactive elements and nutrients from the surface waters into the deep ocean, but also support the bulk of marine heterotrophic microbial production and subsequent food web interactions[8–11]. In addition, the process of assembling DOC into particulate organic carbon (POC) represents a readily available pool of bioreactive and biodegradable organic carbon accessible to the microbial community. Recent studies have demonstrated that marine DOC polymers might contribute significantly to the primary marine aerosols and cloud condensation nuclei over remote areas of the oceans[12–15]. An understanding of assembly dynamics in marine microgels is thus important in the future development of global climate, nutrient transport, and organic carbon transport.

Marine microgels are formed by the aggregation of DOC polymers in a self-assembly fashion followed by further diffusion and annealing. The DOC polymer is generally polyanionic, due to the presence of associated uronic acids and acidic functional groups (such as carboxylate, sulfate, and phosphate)[16,17]. Their negative surface charge can readily chelate ions such as Ca ions, which can play a critical role in crosslinking between polyanionic DOC polymer sites in the marine environment[5]. Other factors influencing aggregation include electrostatic interaction, length of the polymer chains, polymer concentrations, hydrophobic interaction, pH value, temperature, and heterogeneous particles (engineered nanoparticles, ENs)[18–20]. Recent studies have demonstrated that the change in microgel assembly kinetics is induced by ENs (such as plastics and quantum dots) and may be considered a potential disturbance to the marine carbon cycle and bioavailability[20,21]. However, a detailed mechanistic understanding of particle effect on microgel formation, transport, and fate in marine systems, which is important for assessing risk and impact, still remains to be ascertained.

Carbonaceous particles (CNPs), which are generally formed during incomplete combustion of fossil fuels and biomass, continue to increase in the environment as a result of agriculture, industry, permanent deforestation, savanna fires, and motor vehicles[22–24]. Upon their release into the atmosphere, CNPs might serve as condensation nuclei, which are the second largest contributors to climate change[25]. CNPs are of environmental concern for several other reasons as well. For example, CNPs have been identified as a carcinogen and a cause of some respiratory diseases[26]. CNPs can also act as a carrier for pollutants, such as persistent organic pollutants[27], due to

their unique properties, which include a large specific surface area and high affinity for various pollutants. These particles mainly enter the marine system through fluvial discharge and atmospheric deposition. Most CNPs are also commonly regarded as a chemically and biologically stable form of carbon and may persist in the marine or soil system for a long period of time[22,28,29], thus acting as an important sink in carbon cycling[30,31]. While the dissolved organic matter might play an important role in the carbon cycle of the ocean, there is substantial uncertainty regarding the effect of CNPs on the marine DOC pool[22]. In addition, the aggregation and sedimentation of DOC polymers are two interrelated processes that determine the downward flux and the fate of the particles within the marine system.

The objective of this study was to examine the influence of CNPs on the aggregation behavior of marine microgels. Using CB nanoparticles as a model, the aim was to investigate aggregation kinetics and aggregation size as functions of particle concentration. In fact, CB particles are the best model for diesel exhaust particles and urban air pollution particulate matter, as they contain elemental carbonaceous nuclei, which have become an important reference material[32–34]. The addition of electrolytes (NaCl and $CaCl_2$) was used to investigate the mechanism of CB on DOC gel aggregation kinetics. The results of this study will provide new insights into the effect of CNPs on marine microgel formation and facilitate progress in the understanding of the effect of heterogeneous particles on the DOC–POC exchange.

Results

Influence of CB on self-assembly of marine DOC into microgel. The size of the marine DOC microgels (DOC: 2.57 mgL^{-1}) was monitored by DLS for over ten days, as shown in Fig. 1. The marine DOC polymers aggregated spontaneously with second-order kinetics and the size of microgels formed in equilibrium, reached roughly 4–5 μm in 96 hrs (Fig. 1, squares). This result is consistent with previously published observations[5,19]. When CB was added in a concentration of 1 μgL^{-1}, the size of the DOC polymer was significantly smaller than that of the control at 288 hrs (t-test, $p < 0.005$), with the final mean size reaching around 2–3 μm (Fig. 1, circles). As the concentration of CB was increased to 60 μgL^{-1} and 120 μgL^{-1}, the final size of the microgels formed in equilibrium reached around 0.6 μm and 0.45 μm, respectively (Fig. 1, triangles and inverted triangles), which were significantly smaller than those of native marine microgels at 288 hrs (t-test, $p < 0.0001$ and $p < 0.0001$, respectively). The size of the microgels was confirmed by ESEM imaging. Marine DOC samples containing 0, 1, 60, and 120 μgL^{-1} of CB particle were prepared, and ESEM images of microgels collected at 288 hrs were taken. The microgel sizes presented in Figs. 2A–D confirm the DLS measurements (Fig. 1). These data strongly indicate that CB can effectively hinder DOC microgel formation in both the equilibrium size and the formation rate (Table 1), providing convincing evidence that only 1–120 μgL^{-1} of CB released into the aquatic environment can cause a significant change in the self-aggregation of DOC polymers.

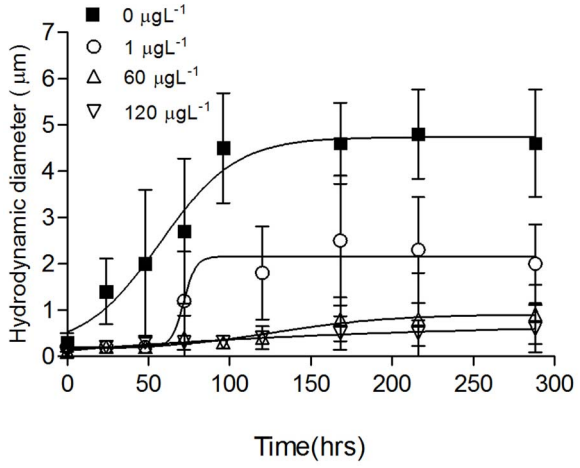

Figure 1 | The influence of CB on the spontaneous assembly of marine DOC polymer was monitored with DLS for over ten days. Different concentrations of CB particles were used, including 0 (squares), 1 (circles), 60 (triangles), and 120 (inverted triangles) μgL^{-1}.

Effects of NaCl and $CaCl_2$ on the self-assembly kinetics of DOC with and without CB particles. As shown in Fig. 3, the self-assembly of marine DOC gel was significantly hindered by adding an extra 1 M of NaCl, which resulted in an equilibrium size of 2–3 μm, compared with 4–5 μm in the control (Fig. 1, squares) at 288 hrs (t-test, $p < 0.005$). Nonetheless, it is noteworthy that the aggregation size of CB–DOC microgels increases with increasing NaCl concentrations: around 0.45 μm without extra NaCl, 1.0–2.6 μm with an extra 0.2 M of NaCl, and 1.3–3.5 μm with an extra 1 M of NaCl. As shown in Fig. 4A, with 10 mM and 20 mM $CaCl_2$, the extra $CaCl_2$ did not have a significant effect upon marine microgel size, yielding 3–4 μm microgels in 120 hrs. The addition of 10 mM of $CaCl_2$ to 120 μgL^{-1} CB–DOC samples led to an increase in the particle size and aggregation rates of DOC polymers, forming ~2 μm in 48 hrs. Further increasing the $CaCl_2$ concentrations to 20 mM resulted in a significant increase in microgel size in the 120 μgL^{-1} CB–DOC samples, forming 3–5 μm microgels (t-test, $p < 0.0001$ compared with no added $CaCl_2$), which was close to the size of native marine microgels (4–5 μm), as illustrated in Fig. 4B. It is noted that the addition of $CaCl_2$ increases the assembly rate constant of CB-DOC. Furthermore, the addition of $CaCl_2$ increased the size and the rate constant more than NaCl (Table 1).

The zeta potential of CB particles and the equilibrium size of CB–DOC microgels. To support the notion that the surface charge of CB might affect the self-assembly of DOC polymers, further evidence of the extent of surface charge interaction can be illustrated by the zeta potential, as shown in Fig. 5. The zeta potential of the CB particles was found to increase with higher concentrations of NaCl and $CaCl_2$. The average zeta potential of the CB particles was raised from −31.3 to −19.57 and −3.53 mV with the addition of 0.2 M and 1 M, respectively, of NaCl. The addition of 0.2 M of NaCl resulted in only a slight reduction in the negative zeta potential of the CB surface, while the addition of 1 M of NaCl further reduced the regime of negative zeta potentials. Compared with NaCl, the average zeta potential was raised remarkably, from −31.3 to 7.07 and 13.16 mV, with the addition of 10 mM and 20 mM, respectively, of $CaCl_2$. It was also found that the equilibrium size of the CB–DOC microgels increased as the zeta potential of CB surface increased.

Discussion

Marine DOC polymers can assemble into ~5 μm microgels; this was first demonstrated by Chin et al.[5]. In the marine carbon cycle, nutrient transportation and microbial processing is greatly influenced by microgel formation. The water chemistry and surrounding particle interaction might exert a significant effect on the aggregation of DOC polymers and stabilization of microgels in the aquatic environment. Understanding the mechanisms of DOC aggregation in the presence of CNPs is therefore essential for assessing the transport and ultimate fate of microgels and CNPs. In this study, using CB nanoparticles as a model particle, the size of DOC microgels was measured under different CNP conditions, concentrations, and electrolytes. Our results revealed that CB can dramatically hinder the formation and kinetics of DOC microgels. The observed decrease in the hydrodynamic diameter of marine CB–DOC might be a result of charge effects con-

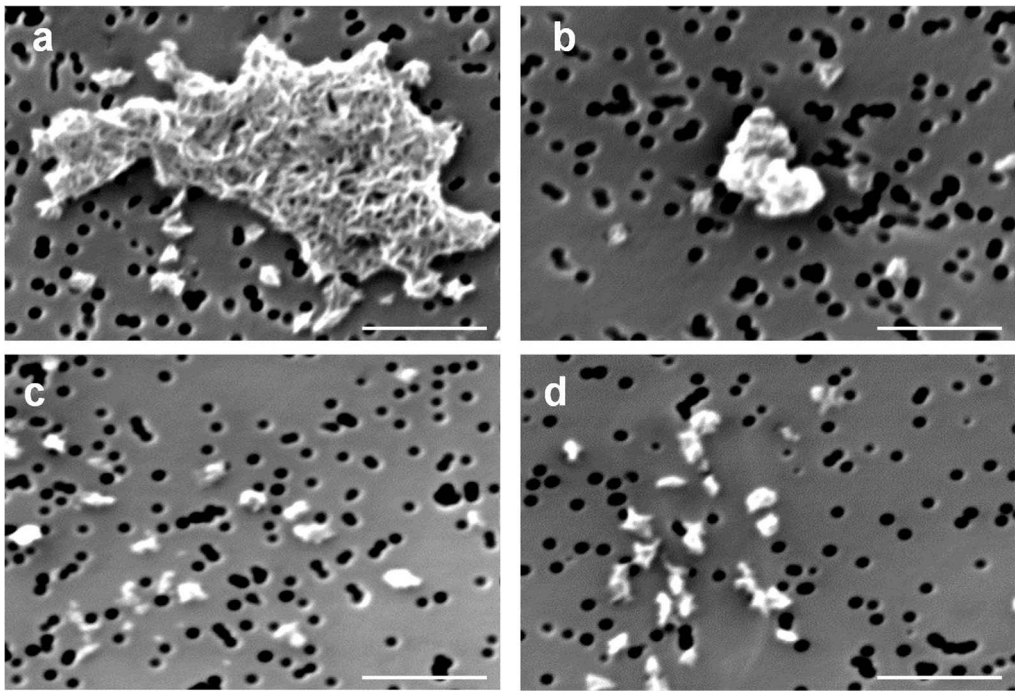

Figure 2 | **ESEM images of marine microgel at different CB particle concentrations: (A)0, (B) 1, (C) 60, and (D) 120 μgL^{-1} (scale bar = 2 μm).**

tributed by the strong negative charges of CB. This observation is consistent with those of other studies, which reported that negatively charged particles were able to decrease the polysaccharide assemblies due to charge stabilization. For instance, negatively charged quantum dots showed a stronger capability for stabilizing EPS in ASW than positively charged quantum dots[21]. The stability of ENs can be increased by coating the surface with negatively charged natural organic matters (NOM)[35]. NOM can also stabilize C_{60} fullerene[36] and metal oxide nanoparticles with negative surface charges[37,38]. Because both CB particles and DOC polymers contain negative surface charges[16,17,39,40], charge stabilization might play an important role in influencing CB on DOC aggregation, as illustrated in Fig. 1.

As discussed above, the negative charges of CB particles effectively can reduce DOC-POC exchange in marine system, which suggests that the cationic charges in native seawater is not enough to screen the strong negative charges of CB particles. Therefore, to investigate the mechanism of the stabilization effects of CB on the DOC gel aggregation kinetics and to assess whether electrostatic interaction is the dominant factor, several electrolytes were used. In the presence of extra NaCl (extra 0.2 and 1 M of NaCl added in native seawater), the size of native marine microgels (the concentration of Na^+ around 0.5 M) was reduced, indicating that the presence of extra NaCl can supply a large number of Na^+ ions surrounding the surface of the DOC polymer and hinder the Ca^{2+} bridges from forming larger assemblies[41]. The key role of the Ca^{2+} bridge in aggregation was demonstrated in the study by Chin et al.[5], wherein removal of Ca^{2+} ions by ethylenediaminetetraacetate (EDTA) significantly prevented polymer assemblies. Nonetheless, the aggregation size of CB–DOC microgels increases with increasing NaCl concentrations. It is thus inferred that the negative charges of CB can be partially neutralized by the extra Na^+ ions that are added, thereby reducing the effect of CB on hindering marine microgel formation (Fig. 3). When investigating the role of Ca^{2+} bridging in the assembly of microgels, it was found that the extra $CaCl_2$ (extra 10 mM and 20 mM added in native seawater, without CB) did not cause significant differences in microgel size, suggesting that Ca^{2+} ions in native seawater (around 10 mM) reach their maximum capacity as cross-linkers for microgel formation (Fig. 4A). When 20 mM of $CaCl_2$ were added to CB–DOC samples, the self-assembly of the CB–DOC microgels increased the microgel size significantly, from 0.45 μm to 4 μm (Fig. 4B). We hypothesize that extra Ca^{2+} can neutralize the negative surface charges of CB, thus reducing the effect of CB on hindering microgel formation. In addition, the microgels were smaller with extra $CaCl_2$ than with extra NaCl. A large number of Na^+ ions surrounding DOC polymers could result in a decrease in the binding efficiency of Ca^{2+}. These inferences are consistent with the variations in zeta potential

Table 1 | The equilibrium size and rate constants of microgel

	Sample	Equilibrium size (μm)	Assembly rate constant (μm^{-1}day^{-1})
CB effect	DOC	4–5	0.0379
	CB (1 μgL^{-1})-DOC	2–3	0.0271
	CB (60 μgL^{-1})-DOC	~0.6	0.0258
	CB (120 μgL^{-1})-DOC	~0.45	0.0179
NaCl effect	DOC + 1 M NaCl	2–3	0.0084
	CB (120 μgL^{-1})-DOC + 0.2 M NaCl	1.0–2.6	0.0050
	CB (120 μgL^{-1})-DOC + 1 M NaCl	1.3–3.5	0.0044
$CaCl_2$ effect	DOC + 20 mM $CaCl_2$	3–4	0.0099
	CB (120 μgL^{-1})-DOC + 10 mM $CaCl_2$	~2	0.0105
	CB (120 μgL^{-1})-DOC + 20 mM $CaCl_2$	3–5	0.0213

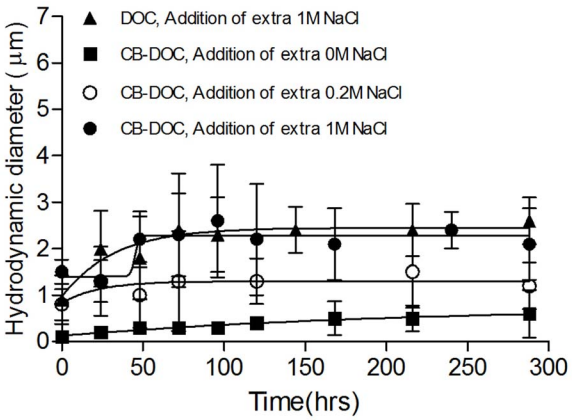

Figure 3 | Effects of NaCl on the self-assembly kinetics of DOC with/without 120 μgL^{-1} of CB particles in seawater. Different concentrations of NaCl added to the CB–DOC sample, including 0 M (squares), 0.2 M (open circles), and 1 M (solid circles), were monitored with DLS for over ten days.

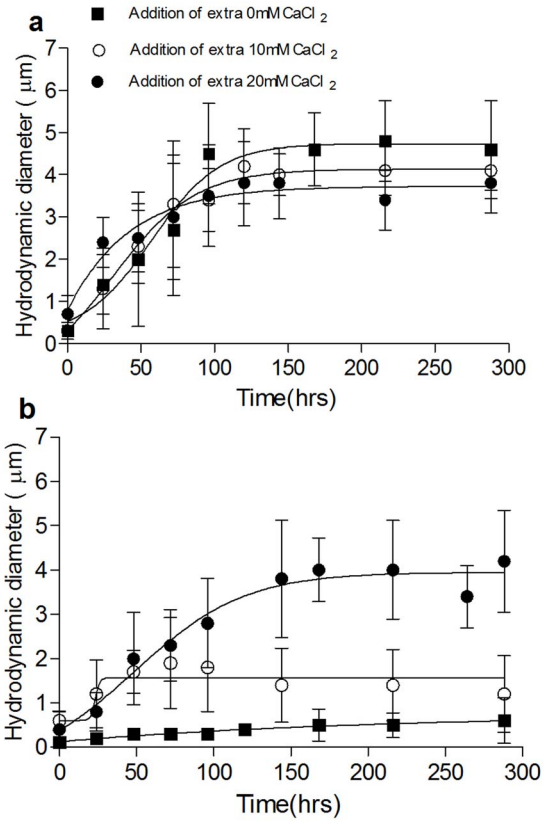

Figure 4 | Effects of extra $CaCl_2$ on the self-assembly kinetics of DOC without (a) and with (b) 120 μgL^{-1} of CB in seawater. Different concentrations of $CaCl_2$ added to the CB–DOC sample, including 0 mM (squares), 10 mM (open circles), and 20 mM (solid circles), were monitored with DLS for over ten days.

and CB–DOC microgel size (Fig. 5). The equilibrium of the marine microgels increased as the CB zeta potential increased. The increases in zeta potential and microgel size were more significant in $CaCl_2$ solution than in NaCl solution, which might be attributed to the specific adsorption of Ca^{2+} on the surface of the CB particles. The greater efficiency of Ca^{2+} in screening the surface charges of CB is consistent with the results obtained by Saleh and Liu[42,43]. Nonetheless, it is noteworthy that the average zeta potential was from −31.3 to −19.57 and 7.07 mV with the addition of 0.2 M of NaCl and 10 mM of $CaCl_2$, respectively, while the equilibrium size did not show significant difference in both experiments (around 1–2 μm), indicating Ca^{2+} and Na^+ can reduce electrical double layer of CB particles but did not have enough Ca^{2+} as cross-linking bridges with DOC polymers. Until 20 mM $CaCl_2$, the aggregate size was substantially increased (close to native marine microgels), possibly due to increased cross-linking bridges through Ca^{2+} bonds (Fig. 5 and 6). Our results clearly demonstrate that electrostatic interaction (Ca^{2+} bonds) plays a critical role in the self-assembly of CB-DOC, which also implies that the self-assembly of marine microgels can be influenced by the surface properties of various natural and anthropogenic particles such as CNPs.

In summary, our results clearly demonstrate that CB can prevent DOC polymers from becoming entangled, due to the negative surface charges of carbonaceous particles prohibiting cross-linking bridges (Fig. 6). The presence of additional electrolytes facilitated the formation of CB–DOC polymer microgels; there was an increase in the assembly rate of CB–DOC polymer aggregation by adding extra $CaCl_2$ (Table 1). Our results show that not only is marine microgel formation driven predominantly by the concentration, hydrophobicity, and length of DOC[18,19], but also that it depends on environmental conditions and surrounding natural or anthropogenic particles[20,44]. The results of this study further suggest that the surface charges of anthropogenic particles can interfere with marine microgel formation. Finally, the environmental implications of our results suggest that CB can dramatically hinder the formation and kinetics of DOC microgels, resulting in a submicron level of "patchiness" in the marine gel phase that could influence the route of DOC–POC exchanges. The small size of the CB particles and DOC gels will reduce the sedimentation flux of organic carbon to the deep ocean, and this portion of organic carbon on the ocean surface might be redistributed into the atmosphere[12]. These negative effects could further change the marine microbial loop, light adsorption[45], and nutrient transportation. Another perspective on the particle effect of DOC–POC is that not only does NOM efficiently affect the stability of natural or engineered particles, but also that microgel formation depends on natural and engineered particles. Further investigation is much needed to explore the complex interactions among DOC, POC, various particles and other environmental parameters (like pH value) that potentially impact the critical organic carbon fluxes in the aquatic environment.

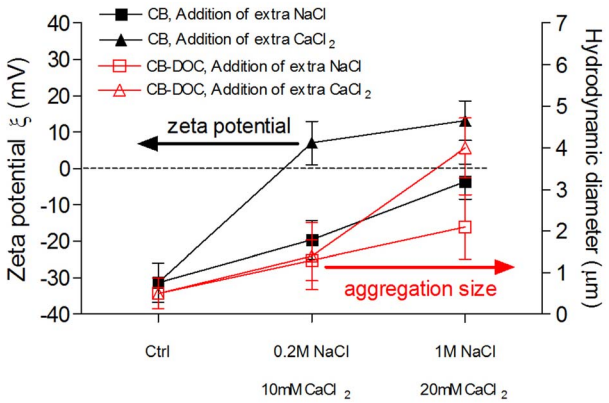

Figure 5 | The zeta potential of CB particles in different ASW, including the addition of NaCl (solid squares) and $CaCl_2$ (solid triangles). Equilibrium size of CB–DOC microgels at varying concentrations of electrolytes, including the addition of NaCl (open squares) and $CaCl_2$ (open triangles).

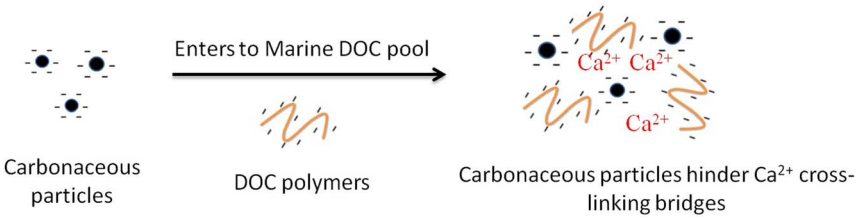

Figure 6 | Interaction between carbonaceous particles and marine DOC polymers.

Methods

Chemicals. American Chemical Society grade reagents, including sodium chloride, potassium chloride, calcium chloride, magnesium chloride, magnesium sulfate, sodium bicarbonate, and dimethyl sulfoxide, were purchased from Sigma Rich (St. Lious, MO). Artificial seawater (ASW: 423 mM NaCl, 9 mM KCl, 9.27 mM $CaCl_2$, 22.94 mM $MgCl_2$, 25.5 mM $MgSO_4$, 2.14 mM $NaHCO_3$) was prepared using deionized (DI) water from a Milli-Q system (Millipore, Billerica, MA) following the protocols established by the Marine Biological Laboratory, Woods Hole, MA (http://www.mbl.edu/BiologicalBulletin/COMPENDIUM/CompTab3.html). CB nanoparticles (Printex 90) with a size of 14 nm and surface area of 300 m^2/g were obtained from Degussa Corporation, Frankfurt, Germany. A stock solution of 60 mg/L CB with 0.005% Tween 20 in DI water was sonicated in an ultrasonicator for 1 hr to ensure the particles were well dispersed. The CB suspension in ASW was monitored by dynamic laser scattering (DLS) for over ten days. We found that the CB particle size under all different ASW conditions was approximately 0.5 μm.

Seawater sampling and pre-treatment. Seawater samples were collected from Friday Harbor, Washington (48.54°N, 123.02°W). The samples were filtered through a 0.22 μm Millipore filter that was pre-washed (0.1 N HCl) and rinsed with Milli-Q water. To inhibit microbial activity, 3 mM sodium azide were added to the seawater samples, which were then stored in the dark at 4°C.

Microgel size measurement. The kinetics of nano- and microgel aggregation has been measured using dynamic laser scattering[5,18–20,45]. Therefore, the aggregate DOC polymer size was monitored by DLS, following protocols presented in[5,46]. In brief, aliquots were poured directly into scattering sample cells. All assembly experiments were monitored for over ten days by analyzing the scattering fluctuations detected at a 45° scattering angle. The autocorrelation function of the scattering intensity fluctuations was averaged over a 12-min sampling time, using a Brookhaven BI 9000AT autocorrelator. Particle size distribution was calculated by following the CONTIN method[5,20]. Calibration of the DLS method was conducted using standard suspensions of latex microspheres (Polysciences, Warrington, PA). Each measurement was replicated ($n \geq 5$) in a 10 ml seawater sample at room temperature.

Zeta potential of CB particle measurement. To measure the surface charges of CB, the zeta potential (ζ) of CB particles was measured with a Brookhaven ZetaPlus (Brookhaven Instruments, Worcestershire, UK) in the presence of NaCl and $CaCl_2$, in varying concentrations, at 25°C. After the data were collected from each sample, the recorded values were averaged.

Environmental scanning electron microscopy (ESEM). Microgels were observed with a FEI Quanta 200 environmental scanning electron microscope (ESEM) (North America NanoPort, Portland, OR). The sample preparation was adopted from[5,19]; briefly, microgel aggregation was filtered through a 0.22 μm Millipore Isopore membrane (Fisher Scientific, Los Angeles, CA). The fixed microgel and CB were dehydrated by soaking them in serially diluted ethanol (35%, 50%, 70%, 95%, and 100% ethanol) for 5 min and then coating them in gold in preparation for viewing with ESEM.

Statistical analysis. The data in this study were presented as means ± standard deviation. Statistically significant differences were based on results of Student's t-test analysis with p values of <0.005 (GraphPad Prism 4.0; GraphPad Software, Inc., San Diego, CA).

1. Chisholm, S. W. Oceanography: stirring times in the Southern Ocean. *Nature* **407**, 685–687 (2000).
2. Falkowski, P. *et al.* The global carbon cycle: a test of our knowledge of earth as a system. *Science* **290**, 291–296 (2000).
3. Hedges, J. I. Global biogeochemical cycles: progress and problems. *Mar. Chem.* **39**, 67–93 (1992).
4. Baines, S. B. & Pace, M. L. The production of dissolved organic matter by phytoplankton and its importance to bacteria: patterns across marine and freshwater systems. *Limnol. Oceanogr.* **36**, 1078–1090 (1991).
5. Chin, W. C., Orellana, M. V. & Verdugo, P. Spontaneous assembly of marine dissolved organic matter into polymer gels. *Nature* **391**, 568–572 (1998).
6. Verdugo, P. *et al.* Marine biopolymer self-assembly: implications for carbon cycling in the ocean. *Faraday Discuss.* **139**, 393–398 (2008).
7. Verdugo, P. Marine microgels. *Annu. Rev. Mar. Sci.* **4**, 375–400 (2012).
8. Kirchman, D. L., Suzuki, Y., Garside, C. & Ducklow, H. W. High turnover rates of dissolved organic carbon during a spring phytoplankton bloom. *Nature* **352**, 612–614 (1991).
9. Kepkay, P. E. Particle aggregation and the biological reactivity of colloids. *Mar. Ecol.-Prog. Ser.* **109**, 293–293 (1994).
10. Carlson, C. A. *et al.* Effect of nutrient amendments on bacterioplankton production, community structure, and DOC utilization in the northwestern Sargasso Sea. *Aquat. Microb. Ecol.* **30**, 19–36 (2002).
11. Verdugo, P. *et al.* The oceanic gel phase: a bridge in the DOM-POM continuum. *Mar. Chem.* **92**, 67–85 (2004).
12. Orellana, M. V. *et al.* Marine microgels as a source of cloud condensation nuclei in the high Arctic. *Proc. Natl. Acad. Sci. U. S. A.* **108**, 13612–13617 (2011).
13. Leck, C. & Bigg, E. K. Aerosol production over remote marine areas-A new route. *Geophys. Res. Lett.* **26**, 3577–3580 (1999).
14. Bigg, E. K. Sources, nature and influence on climate of marine airborne particles. *Environ. Chem.* **4**, 155–161 (2007).
15. Bigg, E. K. & Leck, C. The composition of fragments of bubbles bursting at the ocean surface. *J. Geophys. Res.* **113**, D11209 (2008).
16. Alvarado Quiroz, N. G., Hung, C.-C. & Santschi, P. H. Binding of thorium (IV) to carboxylate, phosphate and sulfate functional groups from marine exopolymeric substances (EPS). *Mar. Chem.* **100**, 337–353 (2006).
17. Kerner, M., Hohenberg, H., Ertl, S., Reckermann, M. & Spitzy, A. Self-organization of dissolved organic matter to micelle-like microparticles in river water. *Nature* **422**, 150–154 (2003).
18. Orellana, M. V. & Verdugo, P. Ultraviolet radiation blocks the organic carbon exchange between the dissolved phase and the gel phase in the ocean. *Limnol. Oceanogr.* **48**, 1618–1623 (2003).
19. Ding, Y.-X. *et al.* Amphiphilic exopolymers from Sagittula stellata induce DOM self-assembly and formation of marine microgels. *Mar. Chem.* **112**, 11–19 (2008).
20. Chen, C. S. *et al.* Effects of engineered nanoparticles on the assembly of exopolymeric substances from phytoplankton. *PLoS One* **6**, e21865 (2011).
21. Zhang, S. *et al.* Aggregation, dissolution, and stability of quantum dots in marine environments: Importance of extracellular polymeric substances. *Environ. Sci. Technol.* **46**, 8764–8772 (2012).
22. Masiello, C. A. New directions in black carbon organic geochemistry. *Mar. Chem.* **92**, 201–213 (2004).
23. Forbes, M. S., Raison, R. J. & Skjemstad, J. O. Formation, transformation and transport of black carbon (charcoal) in terrestrial and aquatic ecosystems. *Sci. Total. Environ.* **370**, 190–206 (2006).
24. Wang, R. *et al.* Global emission of black carbon from motor vehicles from 1960 to 2006. *Environ. Sci. Technol.* **46**, 1278–1284 (2012).
25. Ramanathan, V. & Carmichael, G. Global and regional climate changes due to black carbon. *Nature Geosci.* **1**, 221–227 (2008).
26. Kunzli, N. *et al.* Public-health impact of outdoor and traffic-related air pollution: a European assessment. *Lancet* **356**, 795–801 (2000).
27. Lohmann, R., MacFarlane, J. & Gschwend, P. Importance of black carbon to sorption of native PAHs, PCBs, and PCDDs in Boston and New York harbor sediments. *Environ. Sci. Technol.* **39**, 141–148 (2005).
28. Masiello, C. A. & Druffel, E. R. M. Black carbon in deep-sea sediments. *Science* **280**, 1911–1913 (1998).
29. Jaffé, R. *et al.* Global charcoal mobilization from soils via dissolution and riverine transport to the oceans. *Science* **340**, 345–347 (2013).
30. Aumont, O. *et al.* Riverine-driven interhemispheric transport of carbon. *Glob. Biogeochem. Cycle.* **15**, 393–405 (2001).
31. Dickens, A. F., Gelinas, Y., Masiello, C. A., Wakeham, S. & Hedges, J. I. Reburial of fossil organic carbon in marine sediments. *Nature* **427**, 336–339 (2004).
32. Bockhorn, H. Ultrafine particles from combustion sources: approaches to what we want to know. *Philos. Trans. R. Soc. A-Math. Phys. Eng. Sci.* **358**, 2659–2672 (2000).
33. Medalia, A. I., Rivin, D. & Sanders, D. R. A comparison of carbon-black with soot. *Sci. Total. Environ.* **31**, 1–22 (1983).
34. Heinrich, U. *et al.* Chronic inhalation exposure of wistar rats and two different strains of mice to diesel engine exhaust, carbon black, and titanium dioxide. *Inhal. Toxicol.* **7**, 533–556 (1995).
35. Keller, A. A. *et al.* Stability and aggregation of metal oxide nanoparticles in natural aqueous matrices. *Environ. Sci. Technol.* **44**, 1962–1967 (2010).
36. Xie, B., Xu, Z., Guo, W. & Li, Q. Impact of natural organic matter on the physicochemical properties of aqueous C_{60} nanoparticles. *Environ. Sci. Technol.* **42**, 2853–2859 (2008).

37. Liu, J., Legros, S., von der Kammer, F. & Hofmann, T. Natural organic matter concentration and hydrochemistry influence aggregation kinetics of functionalized engineered nanoparticles. *Environ. Sci. Technol.* **47**, 4113–4120 (2013).
38. Stankus, D. P., Lohse, S. E., Hutchison, J. E. & Nason, J. A. Interactions between natural organic matter and gold nanoparticles stabilized with different organic capping agents. *Environ. Sci. Technol.* **45**, 3238–3244 (2010).
39. Peebles, B. C. *et al*. Physicochemical and toxicological properties of commercial carbon blacks modified by reaction with ozone. *Environ. Sci. Technol.* **45**, 10668–10675 (2011).
40. Xia, T. *et al*. Comparison of the abilities of ambient and manufactured nanoparticles to induce cellular toxicity according to an oxidative stress paradigm. *Nano Lett.* **6**, 1794–1807 (2006).
41. Li, X. *et al*. Cross-Linked polysaccharide assemblies in marine gels: An atomistic simulation. *J. Phys. Chem. Lett.* **4**, 2637–2642 (2013).
42. Saleh, N. B., Pfefferle, L. D. & Elimelech, M. Aggregation kinetics of multiwalled carbon nanotubes in aquatic systems: Measurements and environmental implications. *Environ. Sci. Technol.* **42**, 7963–7969 (2008).
43. Liu, X., Wazne, M., Christodoulatos, C. & Jasinkiewicz, K. L. Aggregation and deposition behavior of boron nanoparticles in porous media. *J. Colloid Interface Sci.* **330**, 90–96 (2009).
44. Kadar, E. *et al*. Chemical interaction of atmospheric mineral dust-derived nanoparticles with natural seawater – EPS and sunlight-mediated changes. *Sci. Total. Environ.* **468–469**, 265–271 (2014).
45. Pace, M. L. *et al*. pH change induces shifts in the size and light absorption of dissolved organic matter. *Biogeochemistry* **108**, 109–118 (2012).
46. Provencher, S. W. & Štêpánek, P. Global analysis of dynamic light scattering futocorrelation functions. *Part. Part. Syst. Charact.* **13**, 291–294 (1996).

Acknowledgments

This work was supported by grants from the National Science Council and the Ministry of Education of Taiwan, ROC, under Contract Numbers NSC 101-2611-M-110-012 and DOE 02C030203. Wei-Chun Chin was supported by grants from the US National Heart, Lung, and Blood Institute (1R15HL095039), US National Science Foundation (CBET-0932404), California Sea Grant (R/CONT-213EPD), and UC CITRIS Program. We gratefully acknowledge critical suggestions from Chi-Shuo Chen, Eric Y-T Chen and Liying Zhao.

Author contributions

R.F.S., C.L.L. and W.C.C. wrote the manuscript. R.F.S., C.L.L. and W.C.C. conceived and designed the experiments. R.F.S. performed the experiments and analyzed data.

Additional information

Competing financial interests: Dr. Wei-Chun Chin (co-author of this manuscript) is a member of the editorial board of Scientific Reports. This does not alter the authors' adherence to all the Scientific Reports policies on sharing data and materials.

How to cite this article: Shiu, R.-F., Chin, W.-C. & Lee, C.-L. Carbonaceous particles reduce marine microgel formation. *Sci. Rep.* **4**, 5856; DOI:10.1038/srep05856 (2014).